PUBLISHED VERSION

Mohammad Albitar, Mohamed Ali, Phillip Visintin, Olivier Lavigne and Erwin Gamboa
Bond stress between reinforcement bars and fly ash-based geopolymer concrete
Proceedings of The 11th fib International PhD Symposium in Civil Engineering, 2016 / Maekawa, K., Kasuga, A., Yamazaki, J. (ed./s), pp.543-550.

This publication is available on Internet under the following Creative Commons license. Some rights reserved. Published: http://creativecommons.org/licenses/by-nc-nd/4.0/

Published publication available at: http://concrete.t.u-tokyo.ac.jp/fib_PhD2016/

PERMISSIONS

http://creativecommons.org/licenses/by-nc-nd/4.0/

creative commons

Attribution-NonCommercial-NoDerivatives 4.0 International (CC BY-NC-ND 4.0)

This is a human-readable summary of (and not a substitute for) the license.

Disclaimer

You are free to:

Share — copy and redistribute the material in any medium or format

The licensor cannot revoke these freedoms as long as you follow the license terms.

Under the following terms:

Attribution — You must give appropriate credit, provide a link to the license, and indicate if changes were made. You may do so in any reasonable manner, but not in any way that suggests the licensor endorses you or your use.

NonCommercial — You may not use the material for commercial purposes.

NoDerivatives — If you remix, transform, or build upon the material, you may not distribute the modified material.

No additional restrictions — You may not apply legal terms or technological measures that legally restrict others from doing anything the license permits.

26 October 2016

http://hdl.handle.net/2440/101987

Bond stress between reinforcement bars and fly ash-based geopolymer concrete

Mohammad Albitar[1], Mohamed Ali[1], Phillip Visintin[1], Olivier Lavigne[2] and Erwin Gamboa[2]

[1]School of Civil, Environmental & Mining Engineering,
[2]School of Mechanical Engineering,
The University of Adelaide,
North Terrace, Adelaide, South Australia (5005), Australia

Abstract

Geopolymer concrete is an innovative construction material that utilises industrial by-product materials, such as fly ash and slags to form a cement replacement for concrete manufacture. In order to simulate the behaviour of all types of reinforced concrete at all load levels, an understanding of the bond between the reinforcement and the concrete is required. This study involves 102 pullout test specimens with bar diameters of 12 to 16mm, concrete cover-to-diameter (C_c/d_b) ratios of 2, 3, 5.8 and 7.8, compressive strength of 33, 38 and 43MPa and a reinforcement corrosion level ranging from 0 to 85% in mass loss. The results show that the bond between the reinforcement and the geopolymer concrete is stronger than the bond that exists between the reinforcement and ordinary Portland cement (OPC)-based concrete. Hence, existing models for OPC can be used as a lower-bounds estimate for analysis and design. Alternatively, new predictive models for the local bond properties and the bond strength variation with corrosion are presented for geopolymer concrete. The results also show that the influence of the C_c/d_b ratio on the bond strength reduces as the C_c/d_b ratio increases, while the influence of the compressive strength on the bond strength remains virtual. This is because increasing the compressive strength leads to an increase in the bond strength.

1 Introduction

Geopolymer concrete has emerged as an innovative engineering material with the potential to form ordinary Portland cement (OPC)-free concrete for both structural and non-structural applications. Geopolymer concrete—that is, concrete manufactured by activating an alternate silica source with a strong alkali solution (Davidovits 1991)—can be formed from several industrial waste materials, including fly ash (Albitar et al. 2014) and lead smelter slag (Albitar et al. 2015). In order to implement these materials in the real world, certain examinations on a structural level need to be performed. Albitar et al. (2014) studied the mechanical properties and Visintin et al. (2016) studied the shear capacity of fly ash-based geopolymer concrete. Hence, this study will focus on the bond behaviour of fly ash-based geopolymer concrete.

The bond between reinforcement and the surrounding concrete in reinforced concrete (RC) members strongly influences the flexural behaviour at both the serviceability (Visintin et al. 2013) and ultimate (Visintin et al. 2012) limit states, as well as influences the shear capacity (Zhang et al. 2014). That is the bond between the reinforcement and the concrete controls the formation of cracks, crack widths and tension stiffening (Choi and Cheung 1996; Marti et al. 1998; Visintin et al. 2012; Knight et al. 2013; Visintin et al. 2013). Corrosion of reinforcement not only reduces the strength of the reinforced concrete, but also leads to deterioration of the bond which can cause increased deflections and reduced strengths ultimately leading to premature failure. There is; therefore, a strong need to quantify the degradation in bond between reinforcement and concrete such that it can be used to predict the long term performance of a structure.

This paper presents the results of the first comprehensive experimental study in literature on the bond characteristic of geopolymer concrete. The test programme involves 102 pullout tests to quantify the bond between conventional ribbed steel reinforcement and class-F fly ash geopolymer concrete. Importantly this study includes 78 pullout tests to quantify the change in bond properties due to corrosion ranging from 0 to 85% and covers a wide variation in concrete cover-to-bar diameter ratio, which

has been shown by Feng et al. (2015) to be the most significant factor in bond degradation due to corrosion.

Importantly for the more widespread uptake of geopolymer concrete the results of this study show that the bond between reinforcement and geopolymer concrete is equal to or better than that exhibited between reinforcement and OPC concrete suggesting existing bond models may be suitable as a reasonable lower bound approximation for geopolymer concrete.

2 Experimental programme

In order to quantify the durability of the local bond stress-slip (τ/δ) properties between conventional ribbed steel reinforcement and geopolymer concrete, a series of 102 pull tests were conducted on class-F fly ash-based geopolymer concrete. The key parameters chosen for investigation were the concrete cover-to-bar diameter (C_c/d_b) ratio, which was taken as 2, 3, 5.8 and 7.8; the level of corrosion, which ranged between 0% and 85% in mass loss and the compressive strength, which was measured at testing day 33, 38 and 43MPa.

2.1 Pullout test specimens

The details and dimensions of pullout test specimens are presented in *Fig. 1* and *Table 1*. The specimens were designed to satisfy different purposes regarding failure mode. A total of 78 specimens (i.e., specimens 1 to 78) were designed to quantify the change in failure mode from concrete cover splitting to reinforcement pullout as C_c increases. The rest 24 specimens (i.e., specimens 79 to 102) were designed such that splitting failure would not occur.

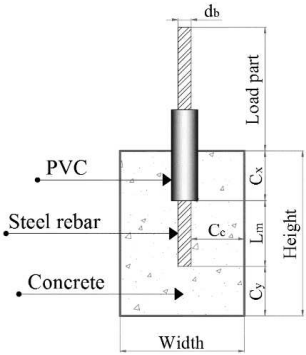

Fig. 1 Sketch of pull-out test specimens.

2.2 Material properties

All pullout test specimens were manufactured from low calcium class-F fly ash as cementitious material, washed river sand and 10mm maximum size of crushed bluestone as fine and coarse aggregates, respectively, and a combination of sodium silicate (Na_2SiO_3) and 10-molar sodium hydroxide (NaOH) as activator solution. Three different compressive strengths were considered, as listed in *Table 2*. Deformed steel bars with two different diameters, 12mm and 16mm, were embedded in the concrete. The average yield strength, f_{sy}, of the steel bar was 560MPa, whereas the average ultimate strength, f_{su}, was 620MPa.

Table 1 Detail of Pullout Test Specimens.

Specimens	f_c (MPa)	Height (mm)	Width (mm)	C_c (mm)	d_b (mm)	L_{se} (mm)	C_x (mm)	C_y (mm)
Specimens: 1, 2, 15, 16, 23, 24, 31, 32, 39, 40, 47, 48	33	200	150	24	12	60	60	80
Specimens: 3, 4, 17, 18, 25, 26, 33, 34, 41, 42, 49, 50	33	200	150	36	12	60	60	80
Specimens: 5, 6	33	200	150	48	12	60	60	80
Specimens 7, 8, 19, 20, 27, 28, 35, 36, 43, 44, 51, 52	33	200	150	32	16	80	60	60
Specimens: 9, 10, 21, 22, 29, 30, 37, 38, 45, 46, 53, 54	33	200	150	48	16	80	60	60
Specimens: 11, 12	33	200	150	64	16	80	60	60
Specimens: 13, 14	33	200	250	177	16	80	60	60
Specimens: 55, 56, 59, 60, 63, 64, 67, 68, 71, 72, 75, 76	43	200	150	24	12	60	60	80
Specimens: 57, 58, 61, 62, 65, 66, 69, 70, 73, 74, 77, 78	43	200	150	36	16	80	60	60
Specimens: 79, 80, 81, 82, 83, 84, 85, 86, 87, 88, 89, 90	38	350	200	94	12	60	120	170
Specimens: 91, 92, 93, 94, 95, 96, 97, 98, 99, 100, 101, 102	38	350	200	92	16	80	120	150

2.3 Accelerated corrosion method

The specimens were fully immersed in a 5% sodium chloride (NaCl) solution and connected to electrochemical system to induce current into the specimens. The electrochemical corrosion method was applied by using direct current supply by connecting the exposed reinforcement to the positive terminal of a constant current to serve as the anode, while the negative terminal of the power source was connected to stainless steel mesh to act as a cathode. The stainless steel mesh was placed inside the solution next to the specimens. The current, i, which was 100 $\mu A/cm^2$, was then passed from the reinforcement bars to the stainless steel.

The magnitude of corrosion was measured using the gravimetric weight-loss. To determine the time of the electrochemical application, the mass loss of reinforcement bar due to corrosion was calculated theoretically according to Faraday's law (*Eq. 1*).

Table 2 Mixture Proportions of Concrete (kg/m^3).

Ingredients	Mixture 1	Mixture 2	Mixture 3
Fly ash	430.11	430.11	430.11
Aggregate (10 mm)	1172.23	1195.56	1182.95
Sand	583.20	588.06	583.20
Sodium hydroxide (14 M)	63.83	63.18	63.83
Sodium silicate	95.75	94.77	95.75
Water	85.05	79.22	74.11
Slump (mm)	250	210	180
Compressive strength (MPa)	33	38	43

$$mass\ loss = \frac{t(s) \times M_{Fr}\left(\frac{g}{mol}\right) \times i\left(\frac{A}{cm^2}\right)}{\rho\left(\frac{g}{cm^3}\right) \times Z \times r\,(cm) \times F\left(\frac{A.S}{mol}\right)} \quad (1)$$

where t is the duration of exposure in seconds, ρ is the density of iron (ρ=7.87g/cm^3), Z is the ionic charge (2 for Fe), r is the radius of corroded bar (cm), F is Faraday's constant (96487 A.S/mol), M_{Fr} is the atomic weight of the metal (55.847g/mol for steel), and i is the average current density in (A/cm^2).

3 Experimental results

3.1 Failure modes

The failure occurred in two different modes. One mode consisted of reinforcing bar slippage due to debonding (*Fig. 2a*), and the other mode consisted of enclosing concrete splitting (*Fig. 2b*). These types of failure are well known from previous studies. The reinforcement bar yield was not observed in the failure mode. The bar slippage mode occurs when sufficient C_c/d_b ratio is provided, whereas splitting failure occurs due to the wedging action of the lugs on the reinforcing bar, which in turn produces pressure that is balanced by circumferential tensile stresses of the concrete. Consequently, splitting cracks are formed due to the stresses, which results in a sudden loss of bond resistance.

(a) Bar slippage.

(b) Enclosing concrete splitting

Fig. 2 Failure modes

3.1 Bond strength

Experimentally recorded bond strength (τ_{max}) of specimens with different corrosion levels are shown in *Fig. 3*, whereas the influence of concrete strength (f_c) is depicted in *Fig.4*. The bond stress (τ) has been determined from *Eq. 2* by assuming the slip is constant over the bonded length.

$$\tau = \frac{P}{\pi \times d_b \times L} \quad (2)$$

where P is the pullout force (N), d_b is the steel bar diameter (mm), and L is the bond length of the steel bar (mm).

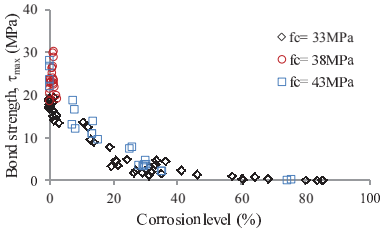

Fig. 3 Bond strength of specimens with different *CL* and f_c.

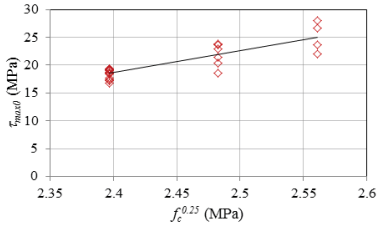

Fig. 4 Relationship between uncorroded bond strength and compressive strength

3.1 Local bond strength-slip relationship

Bond strength degradation due to corrosion can be analysed from the local bond stress-slip (τ/δ) relationship. The full τ/δ relationship of each test is presented in *Figs. 5(a-h)*, where in each graph the variation in the bond properties arises due to the varying corrosion level. The specimens were designated as (specimen number-f_c- d_b-C_c- *CL*).

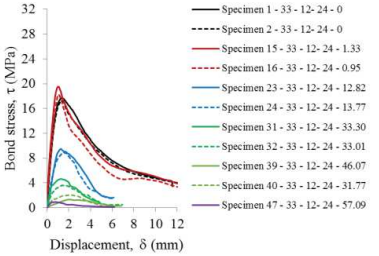

(a) f_c = 33MPa, d_b= 12mm, C_c= 24mm

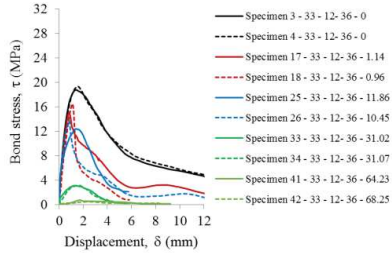

(b) f_c = 33MPa, d_b= 12mm, C_c= 36mm

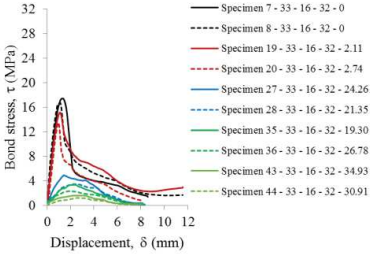

(c) f_c = 33MPa, d_b= 16mm, C_c= 32mm

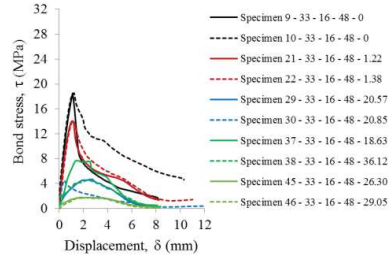

(d) f_c = 33MPa, d_b= 16mm, C_c= 48mm

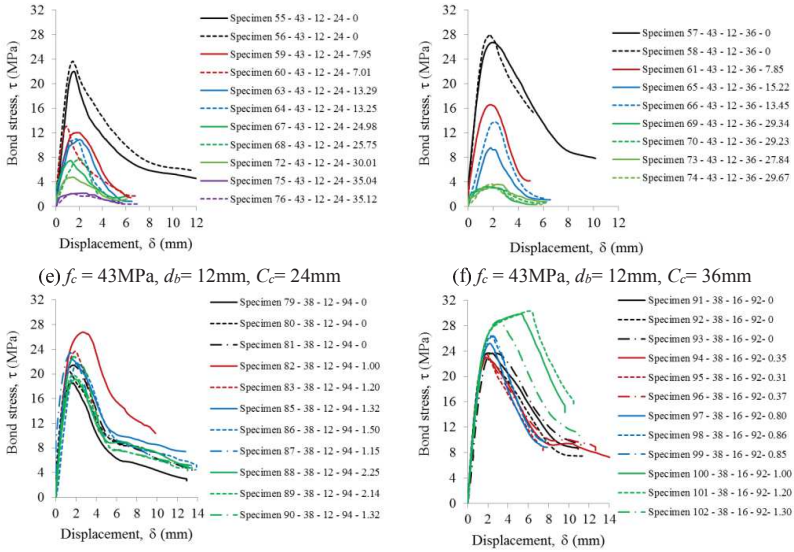

(e) f_c = 43MPa, d_b= 12mm, C_c= 24mm

(f) f_c = 43MPa, d_b= 12mm, C_c= 36mm

(g) f_c = 38MPa, d_b= 12mm, C_c= 94mm

(h) f_c = 38MPa, d_b= 16mm, C_c= 92mm

Fig. 5 Local bond stress-slip relationships of corroded specimens

4 Discussion

4.1 Influence of key parameters on bond strength

The key parameters of the specimens were (i) the steel bar diameter, namely 12mm with rib pitch 7.2mm, and 16mm with rib pitch 9.6mm, (ii) the concrete cover-to-bar diameter (C_c/d_b) ratio of 2, 3, 4, 6, 5.8, and 7.8 for uncorroded specimens, and 2, 3, 5.8, and 7.8 for corroded specimens, (iii) the concrete compressive strength of 33, 38, and 43MPa, and (iv) the corrosion level ranging from 0 to 85% in mass loss. It was found that increasing the compressive strength leads to an increase in the bond strength due to an increase in the bearing, cohesion, and friction strength of the concrete, as observed in *Fig. 4*. Increasing the C_c/d_b ratio was found to result in marginal improvement of the bond strength. The influence of the corrosion level on the bond strength of geopolymer concrete was found to exhibit a similar behaviour to—or even stronger behaviour than—OPC-based concrete, as can be seen in *Fig. 6*, which compares current study geopolymer data with OPC data developed by Feng et al. (2015). It was also found that increasing the corrosion level from 0% to 1% results in an increase in the bond strength due to an increase in the reactionary confinement, which is obtained from the marginal increase in the steel bar. This is because corrosion product 'rust' has a larger volume than steel. Thus, the exerted pressure caused by the development of the expansive corrosion products enhances the mechanical interlocking of the steel bar and the surrounding concrete. Thereafter, the bond strength decreases as the corrosion level increases, because the rust layer, which does not carry any load, acts as a lubricant.

The relationship between the uncorroded bond strength (τ_{max0}) and the compressive strength is expressed through statistical regression as seen in *Eq.3*. It should be noted that the bond strength is considered to be function of the square root of the concrete strength, which is analogous to the tensile capacity of the concrete (Darwin 2005).

$$\tau_{max0} = 39.6 f_c^{0.25} - 76.5 \quad (3)$$

Fig. 6 shows the relationship between the normalised bond strength and the corrosion level. It should be noted that other key parameters were indirectly considered. For example, the dependency of f_c is already accounted for in τ_{max0}, and the influence of C_c/d_b is already allowed for in the *CL*, because the C_c/d_b influences the level of corrosion. Furthermore, *Fig.5* also depicts a comparison between the geopolymer data and the OPC data obtained from Feng et al. (2015). It also presents the proposed model, which can be expressed through statistical regression as

$$\tau_{max}/\tau_{max0} = 0.2CL + 1 \qquad for\ 0 < CL \leq 1 \tag{4}$$

$$\tau_{max}/\tau_{max0} = 1.12e^{-0.065CL} \qquad for\ 1 < CL \leq 85 \tag{5}$$

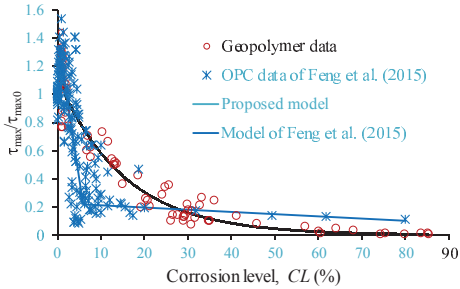

Fig. 6 Comparison between geopolymer and OPC concretes.

4.2 Local bond stress-slip relationship

Bond strength degradation due to corrosion can be analysed from the local bond stress-slip (τ/δ) relationship. For simplification, the bond-slip model can be simplified into two stages (i) slip in ascent stage, and (ii) slip in descent stage (Hai-tao et al. 2012). In theory, any ascending branch can be used (Feng et al. 2015); thus, in the present study the following model is used

$$\tau = \tau_{max}\left(\frac{\delta}{\delta_1}\right)^{\alpha} \tag{6}$$

where δ_1 is the slip at the maximum shear stress τ_{max}, and the value of α can be chosen as 0.4 (CEB-FIP 1993).

For the descending branch, certain values need to be extracted from the τ/δ experimental data, including δ_1, δ_{max}, and τ_{bf}. These values were defined by optimisation, statistical regression and numerical analysis, and will be able to predict them by substituting *Eqs*. 4 and 5.

$$\tau_{bf} = 7.77\left(\tau_{max}/\tau_{max0}\right)^2 - 2.15\,\tau_{max}/\tau_{max0} + 0.69 \tag{7}$$

$$\delta_1 = -0.223\,\tau_{max}/\tau_{max0} + 2 \tag{8}$$

$$\delta_{max} = 0.36\,\tau_{max}/\tau_{max0} + 5.13 \tag{9}$$

4.3 Comparison of Experimental Results with Predictive models

Table 3 summarises the accuracy and precision of *Eqns. 4-9* in predicting the key points of the idealised bond stress slip relationship in *Fig. 6*. It can be seen that, in general, the model performs well at predicting the strength parameters, that is τ_{max} and τ_{bf} as well as at predicting the slip parameters δ_1 and δ_{max}. The scatter in these parameters arises due to the difficulty in identifying a single slip corresponding to the peak stress or the frictional resistance.

Table 3. Comparison of Test Results with Predictive Models

	$(\tau_{max})_{exp}/(\tau_{max})_{pre}$	$(\delta_1)_{exp}/(\delta_1)_{pre}$	$(\tau_{bf})_{exp}/(\tau_{bf})_{pre}$	$(\delta_{max})_{exp}/(\delta_{max})_{pre}$
Mean	1.06	1.00	1.01	1.01
Standard Deviation	0.34	0.46	0.28	0.70
COV	0.32	0.46	0.28	0.69

Conclusion

A series of fly ash-based geopolymer concrete pullout specimens were tested to develop models for the prediction of the maximum bond stress. Based on the test results, it was found that specimens with lower compressive strength are more susceptible to concrete splitting. Increasing the compressive strength resulted in an increase in the bearing, cohesion, and friction strength, and hence, an increase in the bond strength. The concrete cover-to-bar diameter (C_c/d_b) ratio did not have a significant influence on the bond strength, especially for larger ratios. The productive model of the bond strength (τ_{max}), which was determined by examining the influence of the corrosion level on the bond strength, agrees well with the experimental data.

References

Albitar, M., Mohamed Ali, M. S., Visintin, P., and Drechsler, M. 2015. "Effect of granulated lead smelter slag on strength of fly ash-based geopolymer concrete." *Construction and Building Materials*, 83:128–135.

Albitar, M., Visintin, P., Mohamed Ali, M. S. and Drechsler, M. 2014. "Assessing behaviour of fresh and hardened geopolymer concrete mixed with class-F fly ash." *KSCE Journal of Civil Engineering*, 19:1445-1455.

CEB-FIP. 1993. *Design of concrete structures*. CEB-FIP-Model-Code 1990', British Standard Institution, London, UK.

Choi, C. K., and Cheung, S. H. 1996. "Tension stiffening model for planar reinforced concrete members." *Computers & Structures* 59:179–190.

Darwin, D. 2005. "Tension development length and lap splice design for reinforced concrete members." *Progress in Structural Engineering and Materials* 7:210–225.

Davidovits, J. 1991. "Geopolymers: Inorganic polymeric new materials." *Journal of Thermal Analysis* 37:1633−1656.

Feng, Q, Visintin, P. and Oehlers, D. J. 2015. "Deterioration of bond-slip due to corrosion of steel reinforcement in RC." *Magazine of Concrete Research*, in press.

Hai-tao, L., Deeks, A. J., Xiao-zu, S. U. and Dong-sheng, H. 2012. "Tensile bond anchorage properties of Australian 500N steel bars in concrete." *Journal of Central South University of Technology* 19:2718−2725.

Knight, D., Visintin, P., Oehlers, D., and Jumaat, M. 2013. "Incorporating Residual Strains in the Flexural Rigidity of RC members with Varying Degrees of Prestress and Cracking." *Advances in Structural Engineering* 16:1701−1718.

Marti, P., Alvarez, M., Kaufmann, W., and Sigrist, V. 1998. "Tension chord model for structural concrete." *Structural Engineering International* 8:287−298.

Visintin, P., Oehlers, D. J., Haskett, M. 2013. "Partial-interaction time dependent behaviour of reinforced concrete beams." *Engineering Structures*, 49:408−420.

Visintin, P., Oehlers, D. J., Wu, C., and Griffith, M. C. 2012. "The reinforcement contribution to the cyclic behaviour of reinforced concrete beam hinges." *Earthquake Engineering & Structural Dynamics* 41:1591−1608.

Visintin, P., Mohamed Ali, Albitar, M., Wade, L. 2014. "The shear behaviour of geopolymer concrete beams without shear stirrups." *KSCE Journal of Civil Engineering*, in press.

Zhang, T., Visintin, P., Oehlers, D. J., and Griffith, M. 2014. "Presliding shear failure in prestressed RC beams. I: Partial-Interaction mechanism." *Journal of Structural Engineering* 140.